Intersubband gain in a biased superlattice

F. T. Vasko*
NMRC, University College Cork, Lee Maltings, Prospect Row, Cork, Ireland
(Received 3 July 2003; revised manscript received 2 September 2003; published 13 May 2004)

Intersubband transitions in a superlattice under homogeneous electric field is studied within the tight-binding approximation. Since the levels are equipopulated, the nonzero response appears beyond the Born approximation. Calculations are performed in the resonant approximation with scattering processes exactly taken into account. The absorption coefficient is equal zero for the resonant excitation while a negative absorption (in the absence of level repopulation) takes place below the resonance. A detectable gain in the THz spectral region is obtained for the low-doped GaAs-based superlattice and spectral dependencies are analyzed taking into account the interplay between homogeneous and inhomogeneous mechanisms of broadening.

DOI: 10.1103/PhysRevB.69.205309 PACS number(s): 73.21.Cd, 78.45.+h, 78.67.−n

I. INTRODUCTION

The examination of stimulated emission due to intersubband transitions of electrons (monopolar laser effect), which has been carried out during the previous decade, has resulted in mid-IR lasers (see reference in Refs. 1 and 2). Recently, the THz laser has also been demonstrated.[3–6] The standard laser scheme based on vertical transport through the quantum cascade structures, which incorporates the injector and active regions, has been used in both cases. Population inversion appears in the active regions and leads to stimulated emission for the mode propagating along mid-IR or THz waveguide. In contrast to this, the vertical current in a biased superlattice (BSL) with the Wannie-Stark ladder, which appears under the condition $2T \ll \varepsilon_B$[7] (here $\varepsilon_B/\hbar$ is the Bloch frequency and T stands for the tunneling matrix element between adjacent QW's), does not change the populations of the levels. Due to this, the consideration based on the golden rule approach gives a zero absorption. At the same time, for the wide minigap SL, with the width $2T \gg \varepsilon_B$, a negative differential conductivity, i.e., gain due to Bloch oscillations, takes place.[8] This contradiction and the question about THz gain without inversion are discussed in Ref. 9, which is based on the simplified approaches; see Eq. (15) below. In addition, agreement between the numerical results for the wide-miniband and hopping regimes of high-frequency response was noted in Ref. 10.

Since there is no well-defined dispersion relation between energy and momentum, ε and $\mathbf{p}$, beyond the Born approximation, one has to consider the intersubband transitions based on the spectral density function, $A_\varepsilon(\mathbf{p})$, which is a finite-width peak.[11] Let us consider first the two-level model with an identical distribution function for both levels, f_ε. We take into account the off-resonant transitions in the rotating wave approximation with a nonzero detuning energy $\Delta\varepsilon = \hbar\omega - \varepsilon_B$ with respect to the level splitting energy, ε_B, as it is shown in Fig. 1(a). As is clear from the scheme of transitions in Fig. 1(b), the intersubband absorption is given by

$$\alpha_{\Delta\varepsilon} \propto \int \frac{d\mathbf{p}}{(2\pi\hbar)^2} \int_{-\infty}^{\infty} d\varepsilon A_\varepsilon(\mathbf{p}) A_{\varepsilon-\Delta\varepsilon}(\mathbf{p}) (f_{\varepsilon-\Delta\varepsilon} - f_\varepsilon). \tag{1}$$

Moreover, the relation $\alpha_{\Delta\varepsilon} \propto \mathrm{sgn}(\Delta\varepsilon)$ is obtained under the replacement $\varepsilon - \Delta\varepsilon \to \varepsilon$. Taking into account that f_ε decreases with ε, one immediately obtains $\alpha_{\Delta\varepsilon} < 0$ if $\Delta\varepsilon < 0$, i.e., a gain appears in the BSL with disorder described beyond the Born approximation. It should be stressed that populations of levels are the same and gain takes place without repopulation of levels. In the Born approximation, when the spectral function is replaced by δ function, one obtains $\alpha_{\Delta\varepsilon} = 0$.

In this paper, we evaluate Eq. (1) for the low-doped BSL taking into account the intrawell scattering processes exactly. Consideration in Sec. II is based on the tight-binding approach, which corresponds to the sequential tunneling picture, the Green's function formalism, and the quasiequilibrium distribution of electrons over the levels with finite broadening. Discussion of spectral dependencies and numerical estimates are performed in Sec. III taking into account the interplay between homogeneous and inhomogeneous mechanisms of broadening. The last section includes a discussion of the approximations used and conclusions.

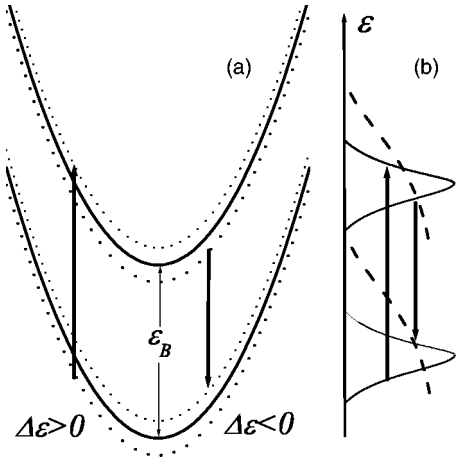

FIG. 1. Off-resonant intersubband transitions (a) and corresponding spectral density functions (b). The dashed curves show distribution functions and arrows indicate the transitions with positive and negative detuning energies.

II. FORMALISM

The intersubband response of a biased SL on a high-frequency electric field is evaluated below taking into account both homogeneous and inhomogeneous mechanisms of broadening. Within the framework of the tight-binding approach we describe the electron states in BSL using the matrix Hamiltonian:

$$\hat{h}_{rr'}=\left(\frac{\hat{p}^2}{2m}+V_{r\mathbf{x}}+r\varepsilon_B\right)\delta_{rr'}+T(\delta_{rr'-1}+\delta_{rr'+1}), \quad (2)$$

where $\hat{p}^2/2m$ is the in-plane kinetic energy operator, m is the effective mass, $V_{r\mathbf{x}}$ is a random potential energy in the rth QW, $r=0,\pm1,\ldots$, which are statistically independent in each QW. The Bloch energy, $\varepsilon_B\simeq|e|FZ$, appears in Eq. (2) due to the shift of levels in the SL with period Z under a homogeneous electric field F; see Ref. 12. The perturbation operator due to a transverse field $[E_\perp\exp(-i\omega t)+\text{c.c.}]$ is written in terms of vector potential as $[\widehat{\delta h}_{rr'}\exp(-i\omega t)+\text{H.c.}]$, where the nondiagonal matrix $\widehat{\delta h}_{rr'}$ is given by

$$\widehat{\delta h}_{rr'}=\frac{ev_\perp}{\omega}E_\perp(\delta_{rr'-1}+\delta_{rr'+1}) \quad (3)$$

and $v_\perp=TZ/\hbar$. The high-frequency current density induced by the perturbation (3), $[I_\omega\exp(-i\omega t)+\text{c.c.}]$, is determined by the standard formula

$$I_\omega=i\frac{2ev_\perp}{L^3}\left\langle\left\langle\sum_r \text{sp}_\parallel(\widehat{\delta\rho}_{r+1r}-\widehat{\delta\rho}_{r-1r})\right\rangle\right\rangle, \quad (4)$$

where 2 is due to spin, $\text{sp}_\parallel\ldots$ is the trace over in-plane motion, $\langle\langle\ldots\rangle\rangle$ is the averaging over random potentials $V_{r\mathbf{x}}$, and L^3 is the normalization volume.

The high-frequency contribution to the density matrix in Eq. (4), $[\widehat{\delta\rho}_{rr'}\exp(-i\omega t)+\text{H.c.}]$, is governed by the linearized equation:

$$-i\omega\widehat{\delta\rho}_{rr'}+\frac{i}{\hbar}(\hat{h}_r\widehat{\delta\rho}_{rr'}-\widehat{\delta\rho}_{rr'}\hat{h}_{r'})+\frac{T}{\hbar}(\widehat{\delta\rho}_{r+1r'}+\widehat{\delta\rho}_{r-1r'}-\widehat{\delta\rho}_{rr'-1}-\widehat{\delta\rho}_{rr'+1})+\frac{i}{\hbar}\widehat{\delta h}_{rr'}(\hat{\rho}_{r'}-\hat{\rho}_r)=0. \quad (5)$$

Here $\hat{h}_r=\hat{p}^2/2m+V_{r\mathbf{x}}+r\varepsilon_B$ describes an in-plane motion in the rth QW and we use the steady state density matrix $(\hat{\rho}_o)_{rr'}\simeq\delta_{rr'}\hat{\rho}_r$, i.e., we have neglected a weak nondiagonal term which is responsible for the tunneling current through the BSL. We restrict ourselves to the consideration of $\propto T^2$ contributions only, so that we can omit $\propto T$ addendums in Eq. (5). Thus, an independent equation for $\widehat{\delta\rho}_r^{(\pm)}\equiv\widehat{\delta\rho}_{r\pm1r}$ takes the form

$$-i\omega\widehat{\delta\rho}_r^{(\pm)}+\frac{i}{\hbar}(\hat{h}_{r\pm1}\widehat{\delta\rho}_r^{(\pm)}-\widehat{\delta\rho}_r^{(\pm)}\hat{h}_r)\simeq-i\frac{ev_\perp}{\hbar\omega}E_\perp(\hat{\rho}_{r\pm1}-\hat{\rho}_r). \quad (6)$$

Note that for the collisionless case $(\hat{\rho}_{r\pm1}-\hat{\rho}_r)\to0$, so that the response vanishes and I_ω is only nonzero due to differences in scattering processes for adjacent QW's. In addition, for the resonant approximation, $|\hbar\omega-\varepsilon_B|\ll\varepsilon_B$, one can neglect the contribution of $\widehat{\delta\rho}_r^{(-)}$.

Writing $\text{sp}_\parallel\ldots$ in Eq. (4) in the coordinate representation, we obtain the current density (4) as $I_\omega=(i2ev_\perp/L^3)\times\langle\langle\Sigma_r\int d\mathbf{x}\delta\rho_r^{(+)}(\mathbf{x},\mathbf{x})\rangle\rangle$. Next, we describe the electron states in the rth QW by the use of the eigenstate problem $(\hat{p}^2/2m+V_{r\mathbf{x}})\psi_{r\mathbf{x}}^\nu=\varepsilon_{r\nu}\psi_{r\mathbf{x}}^\nu$, where a quantum number ν marks an in-plane state. Using this basis, we transform I_ω into

$$I_\omega\simeq i\frac{2ev_\perp}{L^3}\left\langle\left\langle\sum_{r\nu\nu'}\delta\rho_r^{(+)}(\nu,\nu')\int d\mathbf{x}\psi_{r+1\mathbf{x}}^{r\nu}{}^*\psi_{r\mathbf{x}}^{\nu'}\right\rangle\right\rangle \quad (7)$$

and the linearized kinetic equation takes the form

$$(\varepsilon_{r+1\nu}-\varepsilon_{r\nu'}+\varepsilon_B-\hbar\omega-i\lambda)\delta\rho_r^{(+)}(\nu,\nu')=\frac{ev_\perp}{\hbar\omega}E_\perp[f_{\varepsilon_{r+1\nu}}-f_{\varepsilon_{r\nu'}}]\int d\mathbf{x}\psi_{r+1\mathbf{x}}^\nu\psi_{r\mathbf{x}}^{\nu'}{}^*. \quad (8)$$

Here $\lambda\to+0$ and we use the quasiequilibrium distribution $\hat{\rho}_r=f_{\hat{p}^2/2m+V_{r\mathbf{x}}}$, where f_ε is the Fermi function with identical chemical potentials, μ, and temperatures, T_e, for any QW. We introduce the conductivity, σ_ω, according to $I_\omega=\sigma_\omega E_\perp$, and Eqs. (7) and (8) give us

$$\sigma_\omega=i\frac{2(ev_\perp)^2}{\omega L^3}\left\langle\left\langle\sum_{r\nu\nu'}\frac{(f_{\varepsilon_{r+1\nu}}-f_{\varepsilon_{r\nu'}})Q_{r+1,r}^{\nu\nu'}}{\varepsilon_{r+1\nu}-\varepsilon_{r\nu'}+\varepsilon_B-\hbar\omega-i\lambda}\right\rangle\right\rangle, \quad (9)$$

where $Q_{r,r'}^{\nu\nu'}=|\int d\mathbf{x}\psi_{r\mathbf{x}}^\nu{}^*\psi_{r'\mathbf{x}}^{\nu'}|^2$ is the overlap factor. Thus we have evaluated the expression for the resonant response with the scattering processes exactly taken into account.

Below we consider the absorption coefficient introduced according to $\alpha_\omega=(4\pi/c\sqrt{\epsilon})\text{Re}\,\sigma_\omega$, where ϵ is the dielectric permittivity, which is supposed uniform across the structure. In order to perform averaging in Eq. (9), we use the spectral density function in the rth QW determined as $\mathcal{A}_{r,\varepsilon}(\mathbf{x},\mathbf{x}')=\Sigma_\nu\psi_{r\mathbf{x}'}^\nu{}^*\psi_{r\mathbf{x}}^\nu\delta(\varepsilon_{r\nu}-\varepsilon)$,[11] so that $\alpha_{\Delta\varepsilon}$ is written as follows:

$$\alpha_{\Delta\varepsilon}=\frac{2(2\pi ev_\perp)^2}{c\sqrt{\epsilon}\omega L^3}\int_{-\infty}^{\infty}d\varepsilon(f_{\varepsilon-\Delta\varepsilon}-f_\varepsilon)\times\int d\mathbf{x}\int d\mathbf{x}'\sum_r\langle\langle\mathcal{A}_{r+1,\varepsilon}(\mathbf{x},\mathbf{x}')\mathcal{A}_{r,\varepsilon-\Delta\varepsilon}(\mathbf{x}',\mathbf{x})\rangle\rangle \quad (10)$$

with $\hbar\omega\simeq\varepsilon_B$ in the resonant approximation.

We turn now to averaging over short-range and large-scale potentials taking into account that we are considering SL under a homogeneous bias voltage. Due to this the averaged characteristics of scattering processes, both for homogeneous and inhomogeneous mechanisms, do not depend on

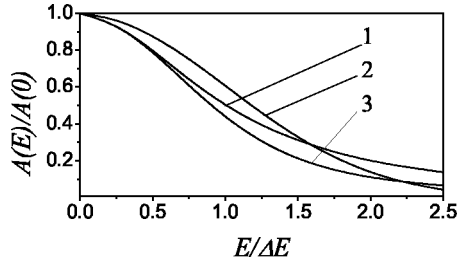

FIG. 2. Transformation of the line shape of $A(E)$ depending on the contributions of different broadening mechanisms: (1) homogeneous broadening, with $\Gamma=0$ and $\Delta E=\gamma$, (2) inhomogeneous broadening, with $\gamma=0$ and $\Delta E=\Gamma$, and (3) both contributions, with $\gamma=\Gamma$ and $\Delta E=\gamma+\Gamma$.

the QW number r. It is convenient to use the Wigner representation and the average of the spectral functions in Eq. (10) takes the form

$$\int\int \frac{d\mathbf{x}d\mathbf{x}'}{L^3}\sum_r \langle\langle \mathcal{A}_{r+1,\varepsilon}(\mathbf{x},\mathbf{x}')\mathcal{A}_{r,\varepsilon-\Delta\varepsilon}(\mathbf{x}',\mathbf{x})\rangle\rangle = \frac{1}{Z}\int \frac{d\mathbf{p}}{(2\pi\hbar)^2}\langle\langle \mathcal{A}_{r+1,\varepsilon}(\mathbf{p},\mathbf{x})\mathcal{A}_{r,\varepsilon-\Delta\varepsilon}(\mathbf{p},\mathbf{x})\rangle\rangle. \quad (11)$$

Here we took into account that $\langle\langle \ldots \rangle\rangle$ does not depend on $\mathbf{x}$ and $L^{-1}\Sigma_r=Z^{-1}$. Performing the averaging over short-range potential, we obtain the spectral function $\langle \mathcal{A}_{r,\varepsilon}(\mathbf{p},\mathbf{x})\rangle = \mathrm{Im}\, G^R_{r,\varepsilon}(p,\mathbf{x})/\pi$ through the retarded Green's written in the Wigner representation as

$$G^R_{r,\varepsilon}(p,\mathbf{x})=(\varepsilon_p-w_{r\mathbf{x}}-\varepsilon-\Sigma)^{-1}. \quad (12)$$

Here $w_{r\mathbf{x}}$ is a large-scale part of potential in the rth QW and Σ is the self-energy function arising from the short-range scattering (see similar calculations in Ref. 13). Below we consider the case of scattering by zero-radius centers when $\mathrm{Im}\,\Sigma$ does not depend on ε, p or $\mathbf{x}$. $\mathrm{Re}\,\Sigma$, which is logarithmically divergent without a small-distance cutoff, is included into the detuning energy $\Delta\varepsilon$, so that the only homogeneous broadening contribution, $-i\gamma$, appears in the denominator of Eq. (12). Performing the averaging over large-scale potentials we write the spectral density, $A(\varepsilon_p-\varepsilon)=\langle\langle \mathcal{A}_{r,\varepsilon}(\mathbf{p},\mathbf{x})\rangle\rangle$, in the integral form:

$$A(E)=\int_{-\infty}^{0}\frac{dt}{2\pi\hbar}e^{i(E-i\gamma)t/\hbar}e^{-(\Gamma t/\hbar)^2/2}+\text{c.c.}, \quad (13)$$

where $\Gamma=\sqrt{\langle w^2_{r\mathbf{x}}\rangle}$ is the inhomogeneous broadening energy. Figure 2 shows how the symmetric spectral density peak [i.e., $A(E)=A(-E)$] changes transforming from a Lorenzian towards a Gaussian lineshape upon an increase in the contribution of the inhomogeneous broadening.

Using the in-plane isotropy of the problem, we finally transform Eq. (10) into

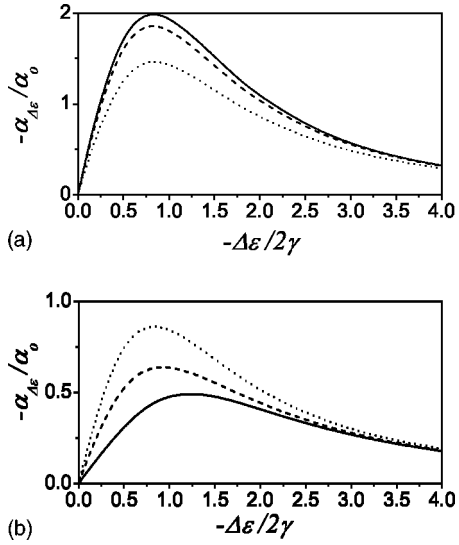

FIG. 3. Dimensionless gain $-\alpha_{\Delta\varepsilon}/\alpha_o$ versus detuning energy $-\Delta\varepsilon/\gamma$ for the homogeneous broadening case ($\Gamma=0$). Panels (a) and (b) correspond to degenerate ($\mu/\gamma=3$) and nondegenerate ($\mu/\gamma=-1$) electrons. Solid, dashed, and dotted curves correspond to $T_e/\gamma=0.3$, 1, and 3, respectively.

$$\alpha_{\Delta\varepsilon}\simeq\alpha_o\int_{-\infty}^{\infty}d\varepsilon\int_0^{\infty}d\xi A(\xi-\varepsilon+\Delta\varepsilon/2)A(\xi-\varepsilon-\Delta\varepsilon/2) \times(f_{\varepsilon-\Delta\varepsilon/2}-f_{\varepsilon+\Delta\varepsilon/2}) \quad (14)$$

with the characteristic absorption, α_o, introduced as follows: $\alpha_o=(e^2/\hbar c)mv_\perp^2/\sqrt{\epsilon}\varepsilon_B Z$. Note, that for the collisionless case the product of spectral functions under the integrals is transformed into $\delta(\xi-\varepsilon+\Delta\varepsilon/2)\delta(\xi-\varepsilon-\Delta\varepsilon/2)$ and one obtains $\alpha_{\Delta\varepsilon}=0$.

III. RESULTS

In this section, we discuss the spectral dependencies $\alpha_{\Delta\varepsilon}/\alpha_o$ given by Eq. (14). Since $\alpha_{\Delta\varepsilon}=-\alpha_{-\Delta\varepsilon}$, we consider only the gain region, $\Delta\varepsilon<0$. It should be noted that the exact description of scattering prosesses distinguishes the calculations performed from Ref. 9. Moreover, the spectral dependencies of Eq. (14) for the homogeneous broadening case ($\Gamma=0$) given by

$$\alpha_{\Delta\varepsilon}\simeq\frac{\alpha_o}{\pi^2}\int_{-\infty}^{\infty}d\varepsilon\int_0^{\infty}d\xi \times\frac{\gamma^2(f_{\varepsilon-\Delta\varepsilon/2}-f_{\varepsilon+\Delta\varepsilon/2})}{[(\xi-\varepsilon+\Delta\varepsilon/2)^2+\gamma^2][(\xi-\varepsilon-\Delta\varepsilon/2)^2+\gamma^2]} \quad (15)$$

do not coincide with Eqs. (19) and (24) in Ref. 9. The double integral over the total and kinetic energies, ε and ξ, remains in Eqs. (14) and (15) while the only summation over momenta was carried out in Ref. 9 because the approach used

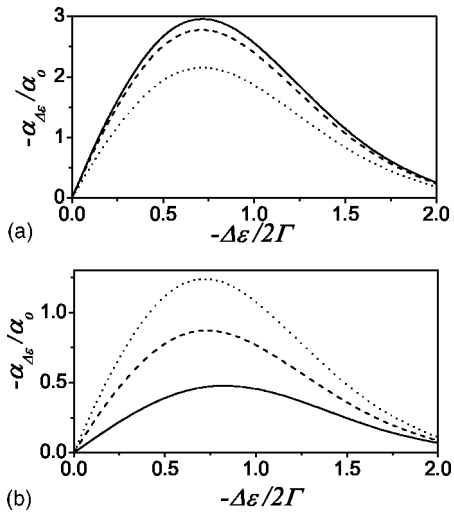

FIG. 4. The same as in Fig. 3 for the inhomogeneous broadening case ($\gamma=0$) depending on parameters μ/Γ and T_e/Γ.

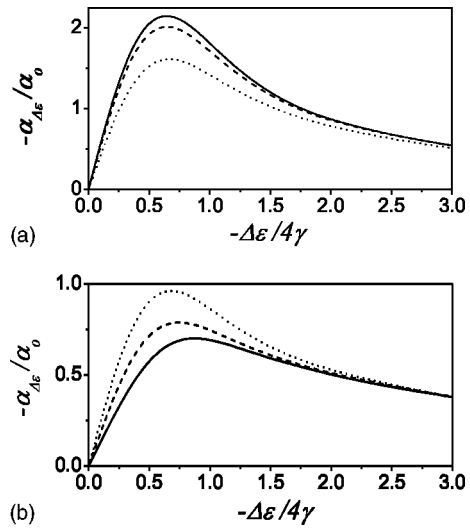

FIG. 5. Dimensionless gain $-\alpha_{\Delta\varepsilon}/\alpha_o$ versus $-\Delta\varepsilon/2(\gamma+\Gamma)$ for the case $\gamma=\Gamma$. Panels (a) and (b) correspond to degenerate ($\mu/2\gamma=3$) and nondegenerate ($\mu/2\gamma=-1$) electrons. Solid, dashed, and dotted curves correspond to $T_e/2\gamma=0.3$, 1, and 3, respectively.

does not take into account the absence of the fixed relation between energy and momentum beyond the Born approximation.[11,14]

First, we examine $\alpha_{\Delta\varepsilon}/\alpha_o$ for the cases of homogenous ($\Gamma=0$) and inhomogeneous ($\gamma=0$) broadening. The dimensionless gain is plotted for the cases of degenerate [Figs. 3(a) and 4(a)] and nondegenerate [Figs. 3(b) and 4(b)] electrons with the concentrations given in Table I. In such calculations we have used the parameters of GaAs/$Al_{0.3}Ga_{0.7}$As-based BSL with the period $Z=15$ nm. The broadening energy, γ or/and Γ is chosen to be 0.5 meV, so that the electron temperature T_e appears to be 1.5–15 K. According to these data, concentration increases with T_e for all cases but the peak gain varies in a different manner: quenching or enhancement of gain occurs for degenerate or non-degenerate electrons respectively. High-energy tails of gain and lower peak values take place for the homogeneous broadening case, when Eq. (13) has a Lorentzian shape. For the inhomogeneous broadening case, $A(E)$ has a Gaussian shape and $\alpha_{\Delta\varepsilon}$ appears to be a sharper function, with a greater maximal value.

In Fig. 5 we present the case $\gamma=\Gamma$, plotting the dimensionless gain versus $\Delta\varepsilon/2(\gamma+\Gamma)$, where $2(\gamma+\Gamma)$ corresponds to the total width of the spectral function (13). One can see both the same style of spectral dependencies and the same temperature/concentration dependencies. Maximal value of gain is founded to be greater for the cases of inhomogeneous or combined broadening.

Next we turn to estimates of the maximal gain for BSL with $T=0.5$ meV, corresponding to the barrier width of 6 nm. For the level splitting energy $\varepsilon_B=10$ meV, which is correspondent to the transverse field $F=6.7$ kV/cm, one obtains $\alpha_o\simeq 6.6$ cm^{-1}, so that the peak gain appears to be between 5 and 20 cm^{-1} for different parameters used in Figs. 3–5. Note, that $\alpha_o\propto T^2$ in the framework of the tight-binding approximation and gain increases rapidly for the narrow barrier case, for example gain exceeds the experimental data,[3] if $T=1$ meV. The density of steady-state tunneling current through the BSL with the above used parameters does not exceed 0.1 kA/cm^2.

IV. CONCLUSIONS

In summary, we have considered the resonant intersubband response of a biased SL and have described gain beyond the Born approximation. Taking into account the interplay between homogeneous and inhomogeneous broadening we have analyzed the spectral and temperature dependencies for the low-doped BSL. The absorption coefficient is equal to zero for the resonant excitation while a detectable gain in the THz spectral region is obtained below the resonance.

Let us discuss the main assumptions used. The tight-binding approach is valid under the condition $\varepsilon_B \gg 2T$ which is satisfied for the numerical estimates performed; note that beyond the Born approximation the broadening can be com-

TABLE I. 3D concentrations, measured in cm^{-3}, versus dimensionless μ and T_e for the cases plotted in Figs. 3 ($\Gamma=0$), 4 ($\gamma=0$), and 5 ($\Gamma=\gamma$).

$T_e/(\gamma,\Gamma)$	$\mu/\gamma=3$, $\Gamma=0$	$\mu/\gamma=-1$, $\Gamma=0$	$\mu/\Gamma=3$, $\gamma=0$	$\mu/\Gamma=-1$, $\gamma=0$	$\mu/2\gamma=3$, $\Gamma=\gamma$	$\mu/2\gamma=-1$, $\Gamma=\gamma$
0.3	3.3×10^{16}	8.8×10^{15}	4×10^{16}	1.6×10^{15}	4×10^{16}	8.2×10^{15}
1	3.4×10^{16}	1.1×10^{16}	4.1×10^{16}	5.4×10^{15}	4.1×10^{16}	1.3×10^{16}
3	4.2×10^{16}	1.5×10^{16}	5.2×10^{16}	2.2×10^{16}	5×10^{16}	3.4×10^{16}

parable with the electron energy determined through μ and T_e. We restrict ourselves to the case of homogeneous field and concentration distributions neglecting a possible domain formation due to the negative differential conductivity at low frequencies.[15] One can avoid instabilities in a short enough BSL because the THz modes propagate in the in-plane directions. In spite of the general expressions (10)–(12) are written through an arbitrary self-energy function Σ, the final calculations were performed for the model included scattering by zero-radius centers and large-scale potential. Such a model describes the interplay between homogeneous and inhomogeneous broadening with the use of statistically independent random potentials in each QW. The Coulomb correlations, which modify the response as the concentration increases, are not taken into account here. This contribution, as well as consideration of intermediate-scale potential, require a special consideration in analogy with the case of a single QW.[16]

To conclude, the simplifications listed do not change either the character of the THz response or the numerical estimates for the gain. It seems likely that this contribution can be found experimentally and more detailed numerical calculations are necessary in order to estimate a potential for applications.

ACKNOWLEDGMENT

This work was supported by Science Foundation Ireland.

*On leave from Institute of Semiconductor Physics, Kiev, NAS of Ukraine, 252650, Ukraine. Email address: ftvasko@yahoo.com

[1] C. Gmachl, F. Capasso, D.L. Sivco, and A.Y. Cho, Rep. Prog. Phys. **64**, 1533 (2001).

[2] C. Sirtori, F. Capasso, J. Faist, A.L. Hutchinson, D.L. Sivco, and A.Y. Cho, IEEE J. Quantum Electron. **34**, 1722 (1998); M. Beck, D. Hofstetter, T. Aellen, J. Faist, U. Oesterle, M. Ilegems, E. Gini, and H. Melchior, Science **295**, 301 (2002).

[3] R. Kohler, A. Tredicucci, F. Beltram, H.E. Beere, E.H. Linfield, A.G. Davies, D.A. Ritchie, R.C. Iotti, and F. Rossi, Nature (London) **417**, 156 (2002).

[4] M. Rochat, L. Ajili, H. Willenberg, J. Faist, H. Beere, G. Davies, E. Linfield, D. Ritchie, Appl. Phys. Lett. **81**, 1381 (2002).

[5] B.S. Williams, H. Callebaut, S. Kumar, Q. Hu, and J.L. Reno, Appl. Phys. Lett. **82**, 1015 (2003).

[6] R. Kohler, A. Tredicucci, F. Beltram, H.E. Beere, E.H. Linfield, A.G. Davies, D.A. Ritchie, S.S. Dhillon, and C. Sirtori, Appl. Phys. Lett. **82**, 1518 (2003).

[7] S. Ktitorov, G. Simin, and V. Sindalovskii, Sov. Phys. Solid State **13**, 1872 (1971); A. Ignatov and Y. Romanov, Phys. Status Solidi B **73**, 327 (1976).

[8] Y. Shimada, K. Hirakawa, M. Odnoblioudov, and K.A. Chao, Phys. Rev. Lett. **90**, 046806 (2003).

[9] H. Willenberg, G.H. Dohler, and J. Faist, Phys. Rev. B **67**, 085315 (2003).

[10] A. Wacker, Phys. Rep. **357**, 86 (2002); Phys. Rev. B **66**, 085326 (2002); in principle, the general formulas presented make possible a description of the gain without inversion for the homogenous broadening case.

[11] G.D. Mahan, *Many-Particle Physics* (Plenum, New York, 1990).

[12] F.T. Vasko and A.V. Kuznetsov, *Electron States and Optical Transitions in Semiconductor Heterostructures* (Springer, New York, 1998).

[13] F.T. Vasko and E.P. O'Reilly, Phys. Rev. B **67**, 235317 (2003).

[14] Using Eq. (24) of Ref. 9 and parameters from Figs. 3(a) and 3(b) one may obtain an essential numerical disagreement because peaks appear to be up to two times lower.

[15] A. Wacker, S.J. Allen, J.S. Scott, M.C. Wanke, and A.P. Jauho, Phys. Status Solidi B **204**, 95 (1997); E. Scholl, *Nonequilibrium Phase Transitions in Semiconductors* (Springer, Berlin, 1987).

[16] F.T. Vasko, P. Aceituno, and A. Hernandez-Cabrera, Phys. Rev. B **66**, 125303 (2002); F.T. Vasko, JETP **93**, 1270 (2001).